The Kirchhoff Approximation in diffusive media with arbitrary geometry

Jorge Ripoll[*a], Vasilis Ntziachristos[b], Joe Culver[c], Arjun G. Yodh[c], and Manuel Nieto-Vesperinas[d]
[a] Institute for Electronic Structure and Laser, Foundation for Research and Technology-Hellas, P.O. Box 1527, 71110 Heraklion, Crete, Greece; [b] Center For Molecular Imaging Research, Massachusetts General Hospital & Harvard Medical School, Bldg 149, 13th Street 5406, Charlestown, MA-02129-2060, USA; [c] Department of Physics and Astronomy, University of Pennsylnavia, Philadelphia PA 19104-6089 USA; [d] Instituto de Ciencia de Materiales, Consejo Superior de Investigaciones Cientificas, Campus de Cantoblanco, 28049 Madrid, Spain

ABSTRACT

Due to the fact that the Kirchhoff Approximation (KA) does not involve matrix inversion for solving the forward problem, it is a very useful tool for quickly solving *3D* geometries of arbitrary size and shape. Its potential mainly lies in the rapid generation of Green's functions for arbitrary geometries, which is key to tomography techniques. We here apply it to light diffusion and study its limits of validity, proving that it is a very useful approximation for diffuse optical tomography (DOT). Its use can improve the existing imaging techinques for real time diagnostics in medicine.

Keywords: Tomography; Image reconstruction techniques; Photon migration; Light propagation in tissues; Photon density waves

1. INTRODUCTION

The study of light transport through highly scattering media such as living tissue has been the focus of recent research, mainly due to its application in medical diagnosis [1-9]. This has been motivated by the fact that light offers structural and compositional information, employs non-ionizing radiation, and depends on relatively low cost instrumentation. Imaging with light is possible due to the low absorption of tissue in the 700 to 850nm spectral region, enabling light penetration depths in the order of 4cm. Lately, rigorous mathematical modeling of light propagation in tissue (see Ref. [10] for a review), combined with technological advancements in photon sources and detection techniques, has made possible the application of tomographic principles [11] for imaging with diffuse light. Hence, one of the major subjects in the photon diffusion area has been diffuse optical tomography (DOT) [4-15].

At the moment, powerful numerical methods are available for accurately solving the forward problem [15,22,23] for arbitrary geometries, but these methods are computationally expensive. A fast method is needed for real time diagnostics, that can deal with arbitrary geometries and sizes. A good candidate is the Kirchhoff Approximation (KA), or the so-called tangent-plane method [24]. The KA is a linear method which does not involve matrix inversion, and can be used to generate the sensitivity functions of the system, so that inversion schemes such as algebraic reconstruction techniques (ART) [11,21], amongst others, can be applied. Also, since it generates the complete Green's function for any three-dimensional (*3D*) geometry, it can be used to improve the already existing reconstruction methods that use the Born or Rytov approximations [18,19,21].

In this work we present the theory of the Kirchhoff approximation in the diffusion equation context, and study its limits of validity. We shall present the exact expression for the Green's function for arbitrary diffusive volumes, and from there the KA is introduced, deriving the expression for the approximate Green's function of the system. Finally the limits of validity are studied in terms of the medium size and parameters, showing that these limits are independent on the geometry, and that mainly depend on the size of the system in diffusion length units.

* jripoll@iesl.forth.gr; http://esperia.iesl.forth.gr/~jripoll

Photon Migration, Optical Coherence Tomography, and Microscopy, Stefan Andersson-Engels, Michael F. Kaschke, Editors, Proceedings of SPIE Vol. 4431 (2001) © 2001 SPIE · 1605-7422/01/$15.00

2. THEORY: EXACT EXPRESSION FOR THE GREEN'S FUNCTION

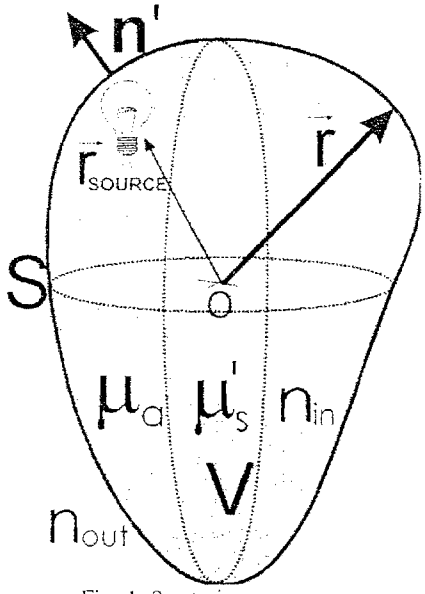

Fig. 1. Scattering geometry

Let us consider the geometry shown in Fig. 1 where we have a diffusive volume V delimited by surface S, which separates it from an outer non-diffusive medium of refractive index n_{out}. This diffusive medium is characterized by its absorption coefficient μ_a, the diffusion coefficient $D = 1/3\mu_s'$ (where μ_s' is the reduced scattering coefficient), and the refractive index n_{in}. If in such a medium the light source is modulated at a frequency ω, the average intensity $U(\mathbf{r},t) = U(\mathbf{r})\exp[-i\omega t]$ represents a diffuse photon density wave (DPDW) [1] and obeys the Helmholtz equation with a wave number $\kappa = (-\mu_a / D + i\omega / cD)^{1/2}$, where c is the speed of light in the medium. In an infinite geometry, the homogenous Green's function g is obtained from:

$$\nabla^2 g(\kappa|\mathbf{r}_s - \mathbf{r}_d|) + \kappa^2 g(\kappa|\mathbf{r}_s - \mathbf{r}_d|) = -4\pi\delta(\mathbf{r}_s - \mathbf{r}_d), \tag{1}$$

and its solution in *3D* is:

$$g(\kappa|\mathbf{r}_s - \mathbf{r}_d|) = \frac{\exp[i\kappa|\mathbf{r}_s - \mathbf{r}_d|]}{|\mathbf{r}_s - \mathbf{r}_d|}. \tag{2}$$

In terms of the *complete* Green's function $G(\mathbf{r}_s, \mathbf{r}_d)$, i.e. taking into consideration the geometry, the average intensity at a point $\mathbf{r}_d$ inside the medium is defined as:

$$U(\mathbf{r}_d) = \frac{1}{4\pi}\int_V \frac{S(\mathbf{r}')}{D} G(\mathbf{r}', \mathbf{r}_d)\mathbf{dr}', \quad \mathbf{r}_d \in V \tag{3}$$

where $S(\mathbf{r}')$ is the source term, and V is the volume occupied by the diffusive medium. In infinite space we of course have $G(\mathbf{r}_s, \mathbf{r}_d) = g(\kappa|\mathbf{r}_s - \mathbf{r}_d|)$.

The general solution to Eq. (1) inside the diffusive medium can be expressed in terms of a surface integral by means of Green's Theorem (see Refs. [23,25] for a detailed derivation) as:

$$G(\mathbf{r}_s, \mathbf{r}_d) = g(\kappa|\mathbf{r}_s - \mathbf{r}_d|) - \frac{1}{4\pi}\int_S \left[G(\mathbf{r}_s, \mathbf{r}') \frac{\partial g(\kappa|\mathbf{r}' - \mathbf{r}_d|)}{\partial \hat{\mathbf{n}}'} - g(\kappa|\mathbf{r}' - \mathbf{r}_d|) \frac{\partial G(\mathbf{r}_s, \mathbf{r}')}{\partial \hat{\mathbf{n}}'} \right] dS', \tag{4}$$

where $\hat{\mathbf{n}}$ is the surface normal pointing into the non-diffusive medium. The boundary condition between the diffusive and non-diffusive medium [26] is:

$$G(\mathbf{r}_s,\mathbf{r}')|_S = -C_{nd} D\hat{\mathbf{n}}'\cdot\nabla G(\mathbf{r}_s,\mathbf{r}')|_S, \mathbf{r}'\in S \tag{5}$$

where C_{nd} takes into account the refractive index mismatch between both media [26]. Introducing Eq. (5) into Eq. (4) we obtain:

$$G(\mathbf{r}_s,\mathbf{r}_d) = g(\kappa|\mathbf{r}_s-\mathbf{r}_d|) + \frac{1}{4\pi}\int_S\left[C_{nd}D_0\frac{\partial g(\kappa|\mathbf{r}'-\mathbf{r}_d|)}{\partial\hat{\mathbf{n}}'} + g(\kappa|\mathbf{r}'-\mathbf{r}_d|)\right]\frac{\partial G(\mathbf{r}_s,\mathbf{r}')}{\partial\hat{\mathbf{n}}'}dS'. \tag{6}$$

A rigorous solution to Eq. (6) can be found by means of the Extinction Theorem (ET) also called the Boundary Element Method (BEM) by discretising the surface and inverting the resulting matrix (see Ref. [23] and references therein). This method, even though it gives a rigorous solution to the forward problem, is time consuming since it involves matrix inversion, and therefore is also limited to surfaces which do not need too many discretisation points (typically <10000).

3. THE KIRCHHOFF APPROXIMATION

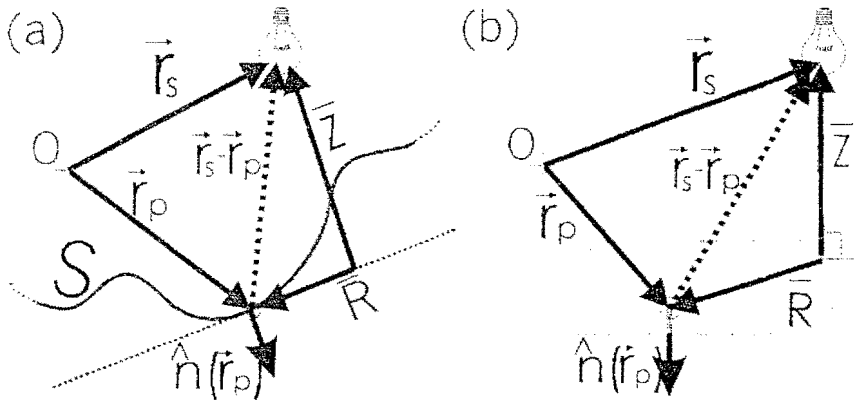

Fig. 2(a). Surface detail of the KA. (b) Representation in the coordinates of the tangent plane.

When many forward solutions need to be generated, such as in most inverse schemes, an approximation to Eq. (6) which can handle *arbitrary* geometries in *3D* in a linear fashion is needed, both for the sake of computing time and memory. One such an approximation is the *Kirchhoff Approximation* (KA), also known as the physical-optics and the tangent-plane method [24]. This approximation assumes that the surface is replaced at each point by its tangent plane. This means that the value of the total intensity U at any point of the surface $\mathbf{r}_p \in S$ is given by the sum of the homogeneous incident field $U^{(inc)}$ and the wave reflected from the *local plane* defined by the surface normal $\hat{\mathbf{n}}(\mathbf{r}_p)$ at that point. In terms of the Green's function this is expressed as:

$$G^{KA}(\mathbf{r}_s,\mathbf{r}_p) = g(\kappa|\mathbf{r}_s-\mathbf{r}_p|)*[1+R_{ND}], \tag{7}$$

where * denotes convolution, and R_{ND} is the reflection coefficient for diffusive waves defined as [27]:

$$R_{ND}(\mathbf{K}) = \frac{iC_{nd}D\sqrt{K^2-\mathbf{K}^2}+1}{iC_{nd}D\sqrt{K^2-\mathbf{K}^2}-1}. \tag{8}$$

In a similar manner, the gradient of the Green's function is:

$$\frac{\partial G^{KA}(\mathbf{r}_s,\mathbf{r}_p)}{\partial\hat{\mathbf{n}}_p} = \frac{\partial g(\kappa|\mathbf{r}_s-\mathbf{r}_p|)}{\partial\hat{\mathbf{n}}_p}*[1-R_{ND}], \tag{9}$$

where the minus sign takes into consideration the different propagation directions of the incident and reflected wave with respect to the local plane. Eqs. (7) and (9) are directly expressed in Fourier space as:

$$G^{KA}(\mathbf{r}_s,\mathbf{r}_p)=\int_{-\infty}^{+\infty}\left[1+R_{ND}(\mathbf{K})\right]\tilde{g}(\mathbf{K},\bar{Z})\exp[i\mathbf{K}\cdot\bar{\mathbf{R}}]d\mathbf{K}\,,$$
$$\frac{\partial G^{KA}(\mathbf{r}_s,\mathbf{r}_p)}{\partial\hat{\mathbf{n}}_p}=\int_{-\infty}^{+\infty}\left[1-R_{ND}(\mathbf{K})\right]\frac{\partial\tilde{g}(\mathbf{K},\bar{Z})}{\partial\bar{Z}}\exp[i\mathbf{K}\cdot\bar{\mathbf{R}}]d\mathbf{K}\,, \tag{10}$$

where $(\bar{\mathbf{R}},\bar{z})$ are the coordinates of $|\mathbf{r}_s-\mathbf{r}_p|$ with respect to the plane defined by $\hat{\mathbf{n}}(\mathbf{r}_p)$ as shown in Fig. 2,

$$\bar{Z}=(\mathbf{r}_s-\mathbf{r}_p)\cdot[-\hat{\mathbf{n}}(\mathbf{r}_p)],$$
$$\bar{\mathbf{R}}=\bar{Z}-(\mathbf{r}_s-\mathbf{r}_p). \tag{11}$$

In Eq. (10) the Fourier transform of the *3D* homogeneous Green's function $\tilde{g}$ is given by [19,29]:

$$\tilde{g}(\mathbf{K},\bar{Z})=\frac{i}{2\pi}\frac{\exp[i\sqrt{\kappa^2-\mathbf{K}^2}\,|\bar{Z}|]}{\sqrt{\kappa^2-\mathbf{K}^2}},$$
$$\frac{\partial\tilde{g}(\mathbf{K},\bar{Z})}{\partial\bar{Z}}=\frac{1}{2\pi}\exp[i\sqrt{\kappa^2-\mathbf{K}^2}\,|\bar{Z}|]. \tag{12}$$

Therefore, if we discretise the surface S in Eq. (6) into N differential areas ΔS, we can write the complete Green's function inside volume V as:

$$G^{KA}(\mathbf{r}_s,\mathbf{r}_d)=g(\kappa|\mathbf{r}_s-\mathbf{r}_d|)+$$
$$\frac{\Delta S}{4\pi}\sum_{p=1}^{N}\left[C_{nd}D\frac{\partial g(\kappa|\mathbf{r}_p-\mathbf{r}_d|)}{\partial\hat{\mathbf{n}}_p}+g(\kappa_0|\mathbf{r}_p-\mathbf{r}_d|)\right]\frac{\partial G^{KA}(\mathbf{r}_s,\mathbf{r}_p)}{\partial\hat{\mathbf{n}}_p}. \tag{13}$$

As seen from Eq. (13), the computation time will increase linearly with the system size. We would like to state that a similar expression to Eq. (13) can be found for diffusive/diffusive interfaces by means of the diffusive/diffusive reflection and transmission coefficients [27].

4. NUMERICAL RESULTS

In order to study the limits of validity of the KA, we shall study the geometry shown in Fig. 3, which consists of a cylinder of radius R with a line source at R_s=R-l_{tr}, where $l_{tr}=1/\mu_s'$ is the transport mean free path. The refractive index inside the diffusive volume is that of water, n_{in}=1.333, and outside that of air, n_{out}=1. An angular scan is performed at $(\rho=R_d, z=0)$ with R_d=R-l_{tr}. So as to quantify the accuracy of the approximation, we shall define the error in percentage as:

$$Error(\%)=100\times\int_{2\pi}\left[1-U^{KA}(R_d,\theta)/U^{ET}(R_d,\theta)\right]d\theta, \tag{14}$$

where U^{ET} is the solution obtained from the Extinction Theorem (ET) [23] using *2D* Green's functions, and U^{KA} is the solution obtained from the KA using a *3D* geometry. In doing so, we wish to show not only the accuracy of the approximation, but to compare computation times between both.

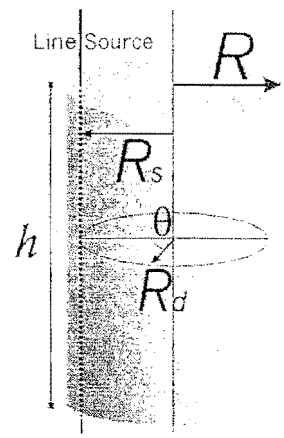

Fig. 3. Geometry used for the numerical simulations.

In all cases, the *KA* results will be generated for a cylinder of height h=10cm and no lids, consisting of N=9191 discretisation points. The results generated with the *ET* in *2D* consisted of N=360. We shall perform the study in the continuous illumination mode (CW), since in this modality light suffers less attenuation. Therefore, the limits of validity here found will apply to all frequency modulation values.

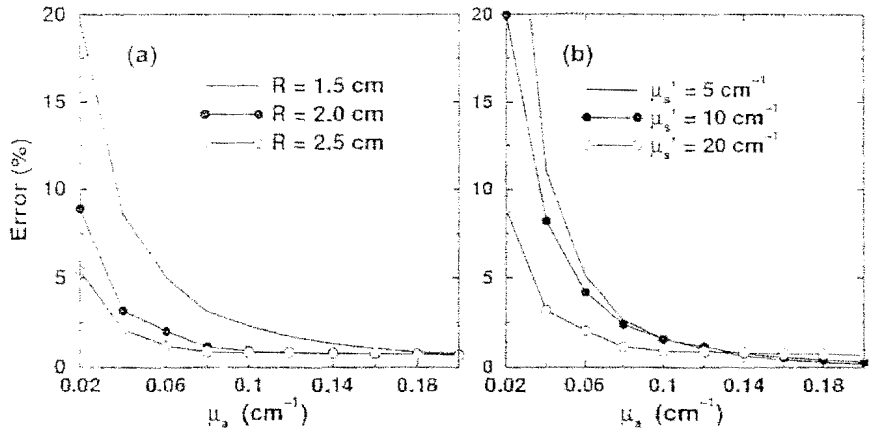

Fig. 4. (a) Error committed in % for different values of μ_a and cylinder radii R. In all cases $\mu_s' = 20\,cm^{-1}$. (b) Same as (a) but for different values of μ_s' for R=2cm.

In Fig. 4 we show the error commited by the KA for different values of R, absorption, and scattering coefficients. The results shown are representative for all possible values. As a general rule, the approximation works well (<5% error) for $R>3L_d$, where L_d is the diffusion length, given in CW by $L_d = \sqrt{D/\mu_a}$. That is, in order to achieve an error of 5% for R=1.5cm, we would have to go to values of $L_d<0.5cm$, which gives $\mu_a>0.7cm^{-1}$ [see Fig. 4(a)]. In the case of diffusive/diffusive interfaces, due to the lower reflectivity the approximation works well for $2R>3L_d$ (similar results where obtained in Ref. [26]).

In order to establish the effect of surface geometry, we have studied the same configuration in Fig. 4, but have added a sine profile of amplitude 0.5cm and period $\pi/4$. The error, Eq. (14), is represented in Fig. 5(a) and compared to the result obtained for a smooth cylinder [Fig. 5(b)]. At this point, we clearly see that when we have shadow regions the approximation fails most. In these regions the approximation tends to give higher values than those expected, since it does not take into consideration obstacles in its path. As shown in Fig. 5(a), errors tend to be <5% except in the shadow areas, and very near the boundaries, where the Green's function has low values due to the boundary conditions which impose it to be zero at the extrapolated distance ($\sim l_{tr}$) from the interface (see Ref. [26]). As shown in Fig. 5(b), when the surface is smooth, the errors are not greater than 5% , and that only very near the interface.

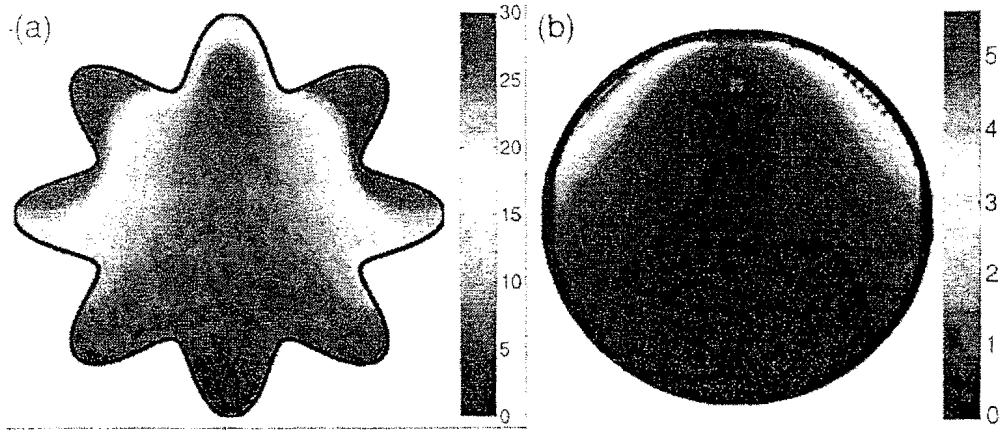

Fig. 5(a). Error comminted in % for a cylinder of R=2.5cm with sine profile of amplitude 0.5cm, and period $\pi/4$, for source locations $(\rho = 1.8cm, \theta = 0)$; (b) Same as but for a smooth cylinder. $\mu_s' = 10\,cm^{-1}$, $\mu_a = 0.1\,cm^{-1}$.

We have tried other values of the period and the ampltiude of the sine profile, finding the same conclusions: as long as we are not in a shadow region, and $R>3L_d$, we are always within a 5% error.

Table I. Comparison of computation times.

Method	*N*	*sources x detectors*	*Total Time*	*Time/N*
KA	9191	9 x 3600	15.7 min.	0.102 sec./point
ET	360	9 x 3600	2.25 min	0.375 sec./point

In Table I we present a comparison of the computation times between the ET in *2D* and the KA in *3D* obtained with a Pentium III at 650MHz, with 250Mb memory. The difference in time is remarkable, but it is most important to consider that the computation time in the ET and any other method which involves matrix inversion, will increase as N^2 in the best of cases, whereas for the KA it increases as N.

5. CONCLUSIONS

We have put forward an approximation to solve *3D* diffusive geometries of arbitrary shape and size in a linear fashion. This approximation has been compared to rigorous results of the diffusion equation, showing that as long as the local size where the detector is placed is $R \geq 3\sqrt{D/\mu_a}$, we are always within a 5% error. This implies that more general Green's functions, which take into account complex geometries, can be used to improve the reconstruction schemes based on Rytov or Born approximations. The computation times of this approximation are very fast compared to the rigorous solution, and increase linearly with the size of the system. We believe this approximation will aid to the development of real time diagnostics with diffuse light in the presence of complex boundaries.

ACKNOWLEDGEMENTS

J. R. acknowledges TMR project #FMRX-CT96-0042 from the EU. V. N. ackwoledges a TMR contract from the EU. This work has received partial support from the Fundacion Ramon Areces.

REFERENCES

1. A.Yodh and B. Chance, "Spectroscopy and imaging with diffusing light", Phys. Today **48**, 38-40, March (1995).
2. S. K. Gayen and R. R. Alfano, "Biomedical imaging techniques", Optics and Photonics news, 17-22, March (1996).
3. E. B. de Haller, "Time-resolved transillumination and optical tomography", J. Biomed. Opt. **1**, 7-17 (1996).
4. M. A. Franceschini, K. T. Moesta, S. Fantini, G. Gaida, E. Gratton, H. Jess, W. W. Mantulin, M. Seeber, P. M. Schlag, and M. Kaschke, "Frequency-domain techniques enhance optical mammography: Initial clinical results", Proc. Natl. Acad. Sci. USA **94**, 6468–6473 (1997).
5. D. Grosenick, H. Wabnitz, H. H. Rinneberg, T. Moesta, and P. M. Schlag, "Development of a time-domain optical mammogram and first *in vivo* applications", Appl. Opt. **38**, 2927–2943 (1999).
6. V. Ntziachristos, and B. Chance, "Probing physiology and molecular function using optical imaging: applications to breast cancer", Rev. in Breast Cancer Res. **3**, 1 (2001).
7. V. Ntziachristos, A. G. Yodh, M. Schnall, and B. Chance "Concurrent MRI and diffuse optical tomography of breast after indocyanine green enhancement", Proc. Nat. Acad. Sci. USA **97**, 2767-2772 (2000).
8. V. Ntziachristos, X. H. Ma, A. G. Yodh, and B. Chance, "Multichannel photon counting instrument for spatially resolved near infrared spectroscopy" Rev. Sci. Instr. **70**, 193–201 (1999).
9. V. Ntziachristos, X. H. Ma, and B. Chance, "Time-correlated single photon counting imager for simultaneous magnetic resonance and near-infrared mammography", Rev. Sci. Instr. **69**, 4221-4233 (1998).
10. S. R Arridge, "Optical tomography in medical imaging", Inv. Prob.**15**, R41-R93 (1999).
11. C. Kak, and M. Slaney, Principles of Computerized Tomographic Imaging (IEEE, New York, 1988).
12. M.A. O'Leary, D. A. Boas, B. Chance and A. G. Yodh, "Experimental images of heterogeneous trubid media by frequency-domain diffusion-photon tomography", Opt. Lett. **20**, 426–428 (1995).
13. P. Gonatas, M. Ishii, J. S. Leigh, and J. C. Schotland, "Optical diffusion imaging using a direct inversion method", Phys. Rev. E **52**, 4361–4365 (1995).
14. M. A. O'Leary, D. A. Boas, X. D. Li, B. Chance, and A. G. Yodh, "Fluorescence lifetime imaging in turbid media", Opt. Lett. **21**, 158–160 (1996).
15. H. Jiang, K. D. Paulsen, U. L. Osterberg, B. W. Pogue, and M. S. Patterson, "Optical image reconstruction using frequency-domain data: simulations and experiments", J. Opt. Soc. Am. A **13**, 253–266 (1996).
16. J. Chang, H. L. Graber, and R. L. Barbour, "Imaging of fluorescence in highly scattering media", IEEE T Bio. Med. Eng. **44**, 810–822 (1997).

17. E. M. Sevick-Muraca, G. Lopez, J. S. Reynolds, T. L. Troy, and C. L. Hutchinson, "Fluorescence and absorption contrast mechanisms for biomedical optical imaging using frequency-domain techniques', Photochem. Photobiol. **66,** 55–64 (1997).
18. V. Ntziachristos, B. Chance, and A. G. Yodh, "Differential diffuse optical tomography", Opt. Exp. **5**, 230–242 (1999). http://www.opticsexpress.org/oearchive/source/12606.htm
19. T. Durduran, J. P. Culver, M. J. Holboke, X. D. Li, L. Zubkov, B. Chance, D. N. Pattanayak and A. G. Yodh, "Algorithms for 3D localication and imaging using near-field diffraction tomography with diffuse light", Opt. Exp. **4**, 247-262 (1999). http://www.opticsexpress.org/oearchive/source/9187.htm
20. Pogue, T. O. McBride, U. Ostenberg, K. Paulsen, "Comparison of imaging geometries for diffuse optical tomography of tissue", Opt. Exp. **4**, 270- (1999). http://www.opticsexpress.org/oearchive/source/9194.htm
21. R. J. Gaudette, D. H. Brooks, C. A. DiMarzio, M. E. Kilmer, E. L. Miller, T. Gaudette, and D. A. Boas, "A comparison study of linear reconstruction techniques for diffuse optical tomographic imaging of absorption coefficient", Phys. Med. Biol. **45**, 1051-1070 (2000).
22. S. R. Arridge, "Photon measurement density functions. Part I: Analytical forms", Appl. Opt. **34**, 7395-7409 (1995).
23. J. Ripoll and M. Nieto-Vesperinas, "Scattering integral equations for diffusive waves. Detection of objects buried in diffusive media in the presence of rough interfaces", J. Opt. Soc. Am. A. **16**, 1453-1465 (1999).
24. P. Beckmann, "Scattering of light by rough surfaces", in *Progress in Optics VI*, E. Wolf, ed. (North-Holland, Amsterdam, 1961), pp. 55-69.
25. M. Nieto-Vesperinas, *Scattering and diffraction in physical optics*, (Pergamon, New York, 1996).
26. R. Aronson, "Boundary conditions for diffusion of light", J. Opt. Soc. Am. A **12**, 2532-2539 (1995).
27. J. Ripoll, V. Ntziachristos, J. P. Culver, D. N. Pattanayak, A. G. Yodh, and M. Nieto-Vesperinas, "Recovery of optical parameters in multiple layered diffusive media: Theory and experiments", J. Opt. Soc. Am. A *in press* (2001).
28. J. Ripoll, M. Nieto-Vesperinas, and R. Carminati, "Spatial resolution of diffuse photon density waves", J. Opt. Soc. Am. A **16**, 1466-1476 (1999).
29. J. Ripoll, and M. Nieto-Vesperinas, "Reflection and trasmission coefficients for diffuse photon density waves", Opt. Lett. **24**, 796-798 (1999).